ACS Macro Letters

Letter

pubs.acs.org/macroletters

Glyco-regioisomerism Effect on Lectin-Binding and Cell-Uptake Pathway of Glycopolymer-Containing Nanoparticles

Pengfei Sun,[†] Yu He,[‡] Mingchang Lin,[†] Yu Zhao,[†] Yu Ding,*[,‡] Guosong Chen,*[,†] and Ming Jiang[†]

[†]The State Key Laboratory of Molecular Engineering of Polymers and Department of Macromolecular Science, Fudan University, Shanghai 200433, China

[‡]School of Life Sciences, Fudan University, Shanghai 200433, China

Supporting Information

ABSTRACT: Sugar regioisomerism (glycosidic linkage on different hydroxyl groups of the same sugar) widely exists in various polysaccharides and glycans with a significant contribution to their biological functions. However, the effects of this regioisomersim in glycopolymers and their self-assembled nanoparticles on such functions were almost not investigated previously. In this paper, this regioisomersim effect is studied for self-assembled nanoparticles **NP-1-Gal** and **NP-6-Gal** from triblock copolymers carrying different constitutional isomers of the pendent sugar species (1 and 6 denote the glycosidic linkage from the anomeric position and 6 position of the galactose unit, respectively). **NP-1-Gal** shows strong binding to lectins of Peanut (*Arachis hypogea*) agglutinin (PNA) and *Erythrina cristagalli* agglutinin (ECA), while **NP-6-Gal** does not. More importantly, they show binding behavior similar to the asialoglycoprotein receptor (ASGPR) but different internalization pathways in the Hep G2 cell after ASGPR-mediated endocytosis; i.e., **NP-1-Gal** can reach the early endosome, late endosome, as well as lysosome, while **NP-6-Gal** enters the early endosome only but not the others.

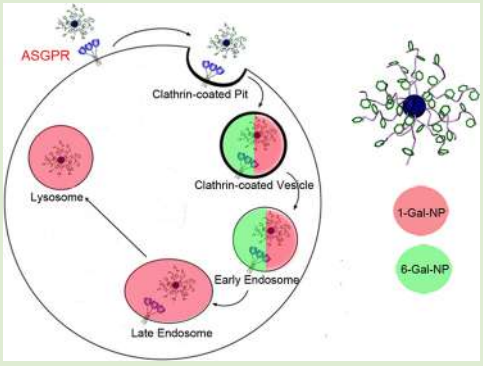

Sugars play fundamental and crucial biological roles in nature. The molecular recognition between sugars and proteins, i.e., lectins, is essential to cell−cell and cell−matrix communication, which is involved in fertilization, virus infection, etc.[1] Most of the sugars participating in these processes exist on the cell surface in the forms of glycoproteins, glycolipids, and proteoglycans, which have a common name "*glycocalyx*". Because of their significant importance and abundance, sugars are known as one of the most important biomacromolecular species just like nucleic acids and proteins. However, our current understanding of the nature and biological roles of sugar is still far behind that of nucleic acid and protein. Probably the most important obstacle in front of us is the extreme complexity of the chemical structures, especially the various isomers in oligosaccharides and polysaccharides.

Meanwhile, it is also well-known that multiple sugar molecules may bind to the same protein together exhibiting an enhanced binding ability, i.e., multivalency.[2] Thus, more and more multivalent neoglycoconjugates have been developed, in which glycopolymer has attracted special attention because of its high molecular weight and versatile synthetic procedure.[3,4] Although the synthesis and lectin-binding assay of many glycopolymers containing monosaccharides or disaccharides in the repeating units have been widely reported,[5] little attention has been paid to the effect of isomerism, e.g., constitutional isomerism of the sugars along the polymer chain on their binding behavior. This effect could be more complicated than anticipated as the multivalency and constitutional isomerism of sugars contribute together to the binding. Considering the substantial role of different sugar isomers and abundance of sugar structures on the cell surface, it is in strong demand to investigate the biological effect of constitutional isomerism in the presence of multivalency, including binding ability to lectins and internalization pathway after cell uptake, which of course is very important for further application of glycopolymers in biorelated areas.

To this goal, self-assembled nano-objects containing glycopolymers with well-defined isomerism on the surface can be the preferred model system. Recently, we reported lectin binding of polymeric vesicles mimicking *glycocalyx*, which were constructed by self-assembled glycopolymers.[6] In the current work, this strategy has been employed by using glycopolymers with the same polymeric backbone but different sugar regioisomers as pendant groups. Thus, we are able to compare the binding ability of the self-assembled nanoparticles with different sugar isomers to lectins in a multivalent manner and the subsequent cell-uptake pathways as well. For this purpose, amphiphilic triblock copolymers containing conjugated polyfluorene (PF) as the middle block and glycopolymer as the side blocks have been designed and prepared, which could assemble into fluorescent nanoparticles with the sugar isomers on the

Received: November 11, 2013
Accepted: December 26, 2013
Published: December 31, 2013

surface. Galactose was taken as a convenient example to build such well-defined constitutional isomers with the glycosidic linkage from its anomeric position (**1-Gal**) or 6-position (**6-Gal**) to the polymeric backbone. Polymer-containing α-mannopyranoside (**1-Man**) was employed as a control (Scheme S1, Supporting Information).

There are a few reports on fluorescent-conjugated glycopolymers for studying carbohydrate−protein interactions. Bunz and co-workers used poly(*p*-phenyleneethynylene)s (PPEs) substituted with α-mannopyranoside side groups to selectively bind lectin concanavalin A (Con A).[7] Liu and co-workers synthesized poly(thiophene)s (PTs)[8] and poly(*p*-phenylene)s (PPPs)[9] with α-mannopyranoside and β-glucopyranoside as side groups, which exhibited similar properties. In these studies, the binding sites, i.e., monosaccharides, were directly connected to the main chains of the conjugated polymers. Thus, fluorescence quench happened when the conjugated polymers were aggregated by the multivalent carbohydrate−protein interactions.[7−10] However, in these works, the effect of isomerism of sugars has not been touched. Our nanoparticles from the triblock copolymers have significant advantages to detect carbohydrate−protein interaction compared to the previous fluorescent conjugated glycopolymers: (1) High water solubility, i.e., as sufficient as 5 mg/mL, can be reached, which allows all of the binding measurements to be readily performed in water. (2) The fluorescent intensity of the nanoparticles keeps stable during their binding to the specific lectins, which ensures further fluorescent labeling in the cell.[11] (3) Multivalent binding tendency is secured because of the abundance of glycopolymer chains on the particle surface. All these features make the nanoparticles serve as a suitable platform to reach our goal of exploring the effect of regioisomerism on the multivalent polymeric scaffold.

The structures of the conjugated block copolymers **PF-1-Gal**, **PF-6-Gal**, and **PF-1-Man** are shown in Figure 1a. Their synthesis started from a conjugated rod-block of poly(9,9-dioctylfluorene) macroinitiator (Scheme S1, Supporting Information) with the bromine-functionalized PF initiator installed at the two ends, which was prepared according to the literature.[12] The macroinitiator had a degree of polymerization (DP) of 6 (Mn = 2.4×10^3 g/mol) by ^{1}H NMR (Figure S1, Supporting Information) and polydispersity (PDI) of 1.4 determined by GPC (Figure S2, Supporting Information). By using atom transfer radical polymerization (ATRP), the side block of poly(glycidyl methacrylate) (PGMA) was initiated directly from the macroinitiator, leading to a coil−rod−coil triblock copolymer[13] (PGMA-*b*-PF-*b*-PGMA) with DP 40 of PGMA determined by ^{1}H NMR (Figure S3, Supporting Information) and PDI 1.4 by GPC (Figure S4, Supporting Information). The total molecular weight of PGMA-*b*-PF-*b*-PGMA was calculated as 1.35×10^4 g/mol ($5.6 \times 10^3 + 2.4 \times 10^3 + 5.6 \times 10^3$), which indicated the weight ratio of the PF as 17%. The subsequent ring opening of the pendent epoxide group of the PGMA block with NaN_3 afforded the side blocks bearing one azide on each methacrylic repeating unit (PAMA-*b*-PF-*b*-PAMA, ^{1}H NMR in Figure S5, Supporting Information), which was further reacted with the sugars modified with alkynes.[14] 1-(2′-Propargyl)-D-galactose (α:β = 10:3) and 1-(2′-propargyl)-α-D-mannose (^{1}H NMR in Figure S6, Supporting Information) were prepared according to the literature[15] and further clicked[14] to PAMA-*b*-PF-*b*-PAMA, which gave **PF-1-Gal** and **PF-1-Man** block copolymers, respectively (^{1}H NMR in Figure S7, Supporting Information). **PF-6-Gal** was prepared according to the literature.[16] The DP of the side blocks of **PF-6-Gal** was 42 determined by its precursor (Mn = 1.6×10^4 g/mol, ^{1}H NMR in Figure S9, Supporting Information) with PDI 1.2 determined by GPC (Figure S10, Supporting Information), which was similar to **PF-1-Gal**.

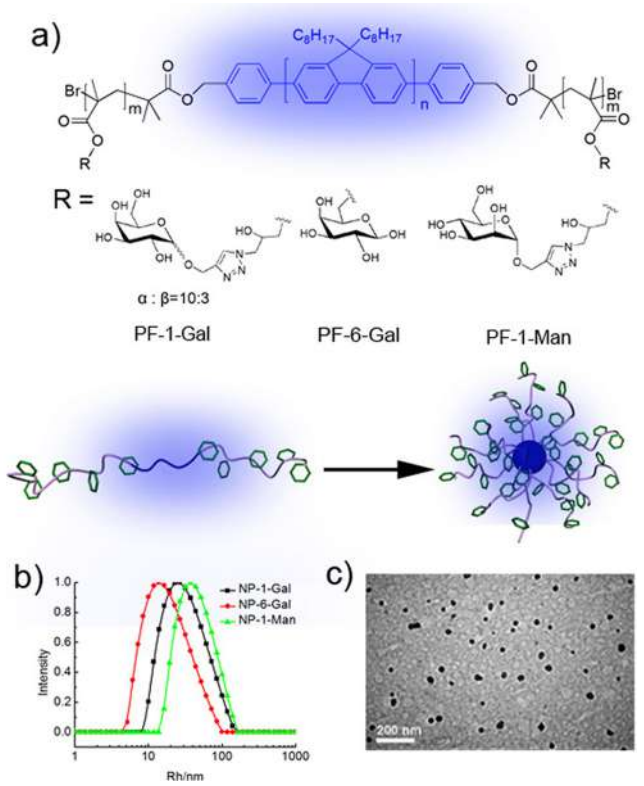

Figure 1. (a) Chemical structures of **PF-1-Gal**, **PF-6-Gal**, and **PF-1-Man** and cartoon representation of the self-assembled nanoparticles. (b) R_h distributions of **NP-1-Gal**, **NP-6-Gal**, and **NP-1-Man** in HEPES buffer at 25 °C (concentration: 0.5 mg/mL). (c) TEM image of **NP-1-Gal**.

With the triblock copolymers **PF-1-Gal**, **PF-6-Gal**, and **PF-1-Man** in hand, which contain the same middle rod block and side coil blocks with similar DP, their self-assembly in water was further performed. Typically, **PF-1-Gal** was solubilized in DMF (1 mg/mL), which was then dialyzed against HEPES buffer for 2 days. Then a certain amount of HEPES buffer was added into the solution to adjust the final concentration to 0.5 mg/mL. The hydrodynamic radius ($\langle R_h \rangle$) was measured to be 23 nm with PDI around 0.21 by dynamic light scattering (DLS) (Figure 1b). From its TEM images, well-dispersed spheres were found from the solution of **PF-1-Gal** (Figure 1c), showing that the polymer self-assembled into nanoparticles with the glyco block as the shell and the rod block as the core, which is denoted as **NP-1-Gal**. Similarly, **NP-6-Gal** ($\langle R_h \rangle$ = 19 nm) and **NP-1-Man** ($\langle R_h \rangle$ = 38 nm) nanoparticles formed via the self-assembly of **PF-6-Gal** and **PF-1-Man**, respectively (Figure 1a and Figure S12, Supporting Information). In short, **NP-1-Gal**, **NP-6-Gal**, and **NP-1-Man** nanoparticles share similar morphology and $\langle R_h \rangle$, which make them nice candidates to evaluate the carbohydrate−protein interactions in the self-assembled state.

Several techniques can be used to investigate the carbohydrate−protein interactions. For the nanoparticles with sugars on the surface, our group utilized DLS to detect the interactions by measuring the binding-induced particle aggregation with multivalent lectins in solution,[6] in which the

dx.doi.org/10.1021/mz400577p | *ACS Macro Lett.* 2014, 3, 96−101

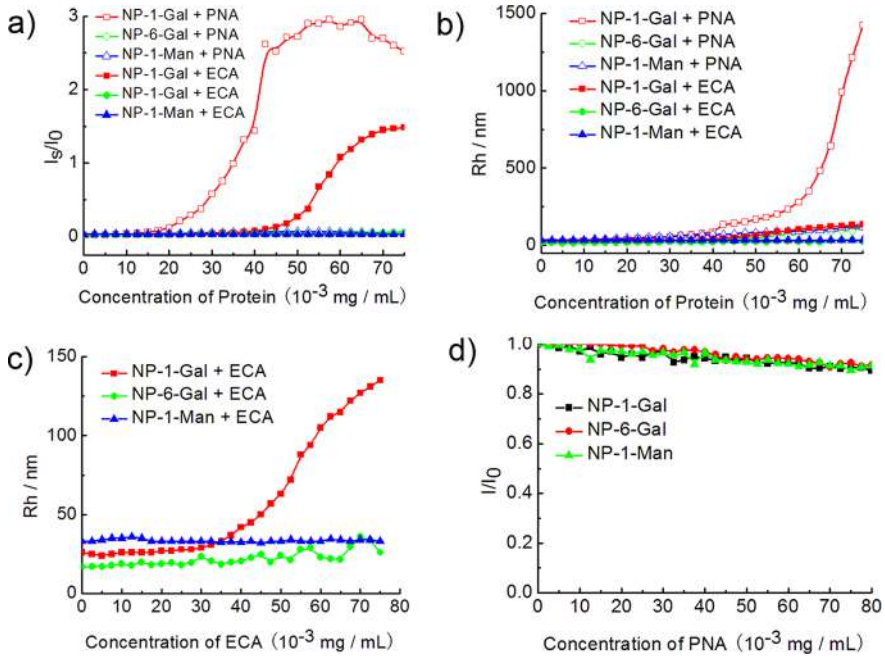

Figure 2. DLS and fluorescence study of the binding behavior between **NP-1-Gal**, **NP-6-Gal**, **NP-1-Man**, and lectins, i.e., PNA and ECA, in HEPES buffer (20 mM, pH 7.4) containing NaCl (50 mM), $CaCl_2$ (5 mM), and $MnCl_2$ (5 mM). (a) Relative scattered light intensity (I_s/I_0) of the three particles after addition of PNA and ECA. (b) $\langle R_h \rangle$ changes of the three nanoparticles after addition of PNA and ECA. (Particle concentration: 0.05 mg/mL). (c) $\langle R_h \rangle$ changes of the particles below 150 nm. (d) Relative fluorescence intensity (I/I_0) of **NP-1-Gal**, **NP-6-Gal**, and **NP-1-Man** with different concentrations of PNA. I_0 is the maximum fluorescent intensity of nanoparticles in the absence of PNA, and I is the maximum fluorescent intensity of nanoparticles after addition of PNA.

relative scattered light intensity (I_s/I_0) was traced as it is generally proportional to the concentration and mass of the macromolecules or particles in solution.[17] By this method, carbohydrate−protein interaction can be detected in solution, which is quite reliable and reproducible, without using fluorescence-labeled proteins. In the present studies, when PNA[18] was added to the solution of **NP-1-Gal** (0.05 mg/mL), a dramatic increase of the scattered light intensity was observed (Figure 2a, red line with circles), as the PNA concentration reached 20 μg/mL. Under the same condition, adding ECA[19] solution to **NP-1-Gal** made an obvious increase of the scattered light intensity as well (Figure 2a, red line with dots). However, with regard to the intensity value at the equilibrium plateau, ECA was only one-half of that with PNA. This may be explained by the tetramer state of PNA and heterodimer state of ECA and each monomer having one sugar-binding site.[19] Meanwhile, $\langle R_h \rangle$ underwent a very sharp increase (Figure 2b) when the concentration of PNA reached 50 μg/mL in the solution of **NP-1-Gal** (0.05 mg/mL). Similarly, after addition of ECA, the $\langle R_h \rangle$ value of **NP-1-Gal** particles (0.05 mg/mL) was increased to around 150 nm (Figure 2c), significantly smaller than that obtained with PNA addition. Moreover, it can be seen that from the scattered light intensity and $\langle R_h \rangle$ **NP-1-Man** and **NP-6-Gal** did not show any binding ability with both PNA and ECA, showing that specific interactions do not exist between these sugar-covered nanoparticles and the two lectins. This result gives clear evidence that **NP-1-Gal** binds to PNA and ECA, while **NP-6-Gal** and **NP-1-Man** do not. Thus in this case the binding ability of the nanoparticles is mainly determined by the constitutional isomerism of sugars, which may be predicted from the crystal structures of lectin and sugar.[18,19] Furthermore, as shown in Figure 2d, successful binding between **NP-1-Gal** and PNA does not induce fluorescence quenching of the nanoparticles; i.e., the fluorescence of **NP-1-Gal** is quite stable during protein titration, which is very different from the previous reports on the interactions between lectin and sugar-containing polymers.[7−9] This result comes from our design of the block copolymer, where the fluorescent species and sugar units exist in different blocks. The aggregation of the nanoparticles due to the interaction between the sugar species and lectins would not affect the PF chain in the core of the nanoparticles. Obviously, such stable fluorescent emission makes the subsequent cell-uptake study of the nanoparticles by fluorescent confocal microscopy realizable.

Besides the plant lectins, some animal lectins are known for their binding ability with galactopyranoside. The most representative one found in animals is the asialoglycoprotein receptor (ASGPR).[20] It is related to the circulation of glycoproteins in our body by selectively removing "old" proteins, which have galactopyranoside exposed at the end of their glycan chain.[21] ASGPR is highly expressed on the hepatic cell surface and induces endocytosis of galactoside-containing glycoproteins after binding. Here the binding ability of **NP-1-Gal**, **NP-6-Gal**, and **NP-1-Man** with human ASGPR was examined by a quartz crystal microbalance (QCM). The surface of a QCM-D sensor was first modified with ASGPR via polyhistidine (His) tag-affinity.[22] Then the frequency changes were monitored in the processes of **NP-1-Gal** and **NP-6-Gal** loading to the sensor surface. As shown in Figure 3, the frequency underwent an obvious decrease in both the cases, indicating that **NP-1-Gal** and **NP-6-Gal** show binding abilities similar to ASGPR, which to some extent can be explained by the previous investigation on monosaccharides or oligosaccharides.[23] As a control experiment, **NP-1-Man** did not show any binding effect to the ASGPR surface.

dx.doi.org/10.1021/mz400577p | *ACS Macro Lett.* 2014, 3, 96−101

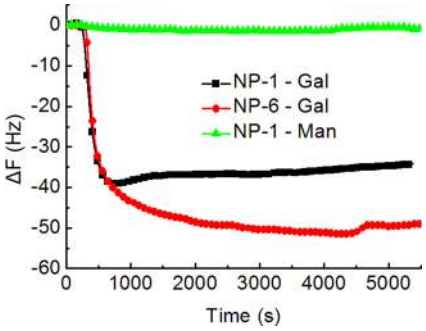

Figure 3. Binding of ASGPR with **NP-1-Gal**, **NP-6-Gal**, and **NP-1-Man** measured by QCM.

The uptake of the two binding nanoparticles by Hep G2 cells with abundantly expressed ASGPR on their surface was further investigated. HeLa cells, which do not express ASGPR, were employed in the assay as a control.[24−27] **NP-1-Gal** and **NP-6-Gal** were first proved with low cytotoxicity in vitro (Figure S13, Supporting Information). Then Hep G2 and HeLa cells were first seeded onto sterile glass coverslips that had been placed in the wells of a 24-well plate and then cultured in 2 mL of DMEM containing 10% FBS overnight. The cells were then incubated with **NP-1-Gal** or **NP-6-Gal** (50 μg) in DMEM for 4 h at 37 °C. After removal of the unbound **NP-1-Gal** or **NP-6-Gal**, fluorescence imaging of cells was carried out using confocal microscopy. As shown in Figure 4a and 4b, the images

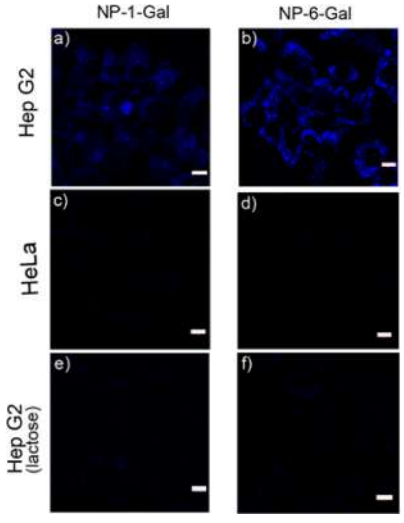

Figure 4. Confocal fluorescence microscopy images of nanoparticles internalized by Hep G2 cells with 50 μg of (a) **NP-1-Gal** or (b) **NP-6-Gal**; HeLa cells with 50 μg of (c) **NP-1-Gal** or (d) **NP-6-Gal**; Hep G2 cells with preincubated 20 mM lactose for 1 h at 37 °C, and then **NP-1-Gal** (e) or **NP-6-Gal** (f) at 37 °C after 4 h incubation. Fluorescence of **NP-1-Gal** and **NP-6-Gal** is blue. Scale bar: 10 μm.

clearly indicate the presence of **NP-1-Gal** and **NP-6-Gal** in the cytoplasm but not in the nuclei of Hep G2 cells (Figure S14c,f, Supporting Information). This internalization was further confirmed with Z-stack images (Figures S15 and S16, Supporting Information), which are the layer cross-sectional images of the focal plane at different levels in cell samples. The uptake of **NP-1-Gal** and **NP-6-Gal** by Hep G2 cells cannot be observed when the incubation was at 4 °C, indicating an energy-dependent internalization process (Figure S17, Supporting Information). Meanwhile, **NP-1-Gal** and **NP-6-Gal** cannot be internalized by HeLa cells (Figure 4c,d and Figure S18, Supporting Information). To confirm that the uptake of **NP-1-Gal** and **NP-6-Gal** results from a specific interaction between galactopyranoside and ASGPR, preincubation of the cells with lactose[26] (as a competitive inhibitor, 20 mM) for 1 h before the incubation with **NP-1-Gal** and **NP-6-Gal** was performed. It resulted in significantly inhibited endocytosis (Figure 4e,f and Figure S18, Supporting Information). Moreover, **NP-1-Man** was used as a control because 1-mannopyranoside does not interact with ASGPR. After incubation of Hep G2 cells with **NP-1-Man** (50 μg) at 37 °C for 4 h, the confocal microscopy result does not show any obvious endocytosis (Figure S14h, Supporting Information).

The internalization pathway of **NP-1-Gal** and **NP-6-Gal** (Figure 5) in Hep G2 was further examined after endocytosis.

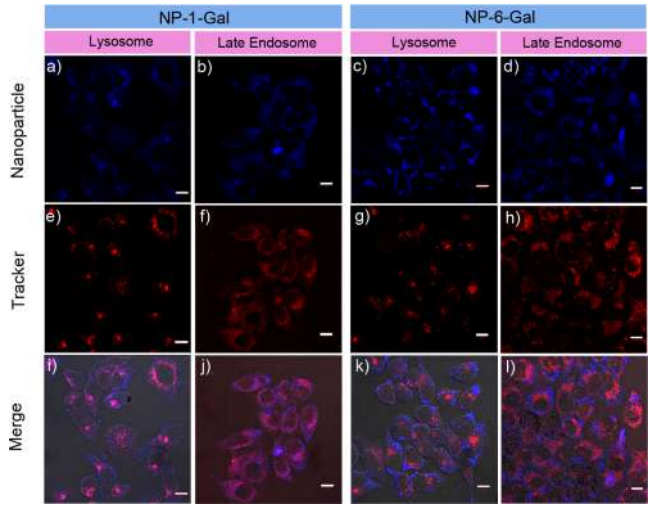

Figure 5. Colocalization of nanoparticles with intracellular compartments: Hep G2 cells were incubated with nanoparticles at 37 °C for 4 h. Confocal micrographs of the cells show (a−d) intracellular location of **NP-1-Gal** and **NP-6-Gal** in blue, (e−h) lysosomes labeled by lysotracker (red) or late endosomes expressing RFP (red), and (i−l) superimposed images. Scale bar: 10 μm.

To further trafficking of endocytotic pathways via different cellular organelles, LysoTracker Red DND-99 was used to label the lysosome, and CellLight Late Endosomes-RFP cell transduction reagent for expression of the red fluorescence protein (RFP) was used to label the late endosome selectively. Confocal microscopy images of **NP-1-Gal** showed the colocalization of blue from the nanoparticle (Figure 5a) and red from LysoTracker (Figure 5e), proving that the nanoparticles are found inside lysosomes (Figure 5i). Similarly, the images also showed the colocalization of blue from the nanoparticle (Figure 5b) and red from RFP in late endosomes (Figure 5f), proving that the **NP-1-Gal** is found inside the late endosome as well (Figure 5j). However, in the case of **NP-6-Gal**, the absence of colocalization between blue from the nanoparticle (Figure 5c,d) and red from LysoTracker (Figure 5g) or red from RFP in the late endosome (Figure 5h) is also apparent in Figure 5k,l, indicating the absence of **NP-6-Gal** in both the lysosome and late endosome. Thus, the difference in localization between **NP-1-Gal** and **NP-6-Gal** inside Hep G2 cells after endocytosis is apparent. Considering that the binding behavior of the nanoparticles to ASGPR seemed similar to that

dx.doi.org/10.1021/mz400577p | *ACS Macro Lett.* 2014, 3, 96−101

observed by QCM, this result was to some extent beyond our expectation and thus inspired us to track back of both **NP-6-Gal** and **NP-1-Gal** inside the cell. The CellLight Early Endosomes−RFP cell transduction reagent was used and resulted in expression of the red fluorescence protein (RFP) in early endosomes. As shown in Figure 6, both **NP-6-Gal** and

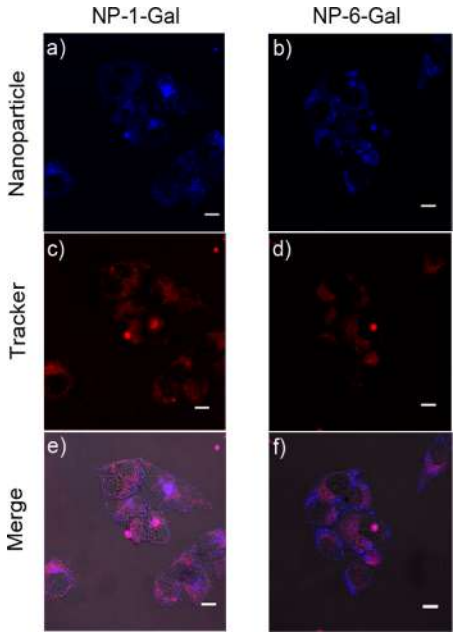

Figure 6. Confocal fluorescence microscopy images show the subcellular of **NP-1-Gal** (a, c, e) and **NP-6-Gal** (b, d, f) within early endosomes of Hep G2 cells. Fluorescence images with blue from nanoparticles **NP-1-Gal** (a) and **NP-6-Gal** (b). (c,d) Fluorescence images with red from early endosomes tracker. (e,f) Merge of the above images in the same column. Scale bar: 10 μm.

NP-1-Gal show colocalization with early endosomes. Because of the general pathway of endocytosis, i.e., from the clathrin-coated vesicle to early endosome, late endosome, and finally lysosome,[1] based on the results above we intend to conclude that **NP-1-Gal** with *1-galactopyranoside* could reach the lysosome via this pathway; however, its counterpart **NP-6-Gal** with constitutional isomer *6-galactopyranoside* could not, which mostly stays in the early endosome within the same or even rather long time scale during incubation. In other words, our results demonstrated the different distributions of **NP-1-Gal** and **NP-6-Gal** after their internalization by Hep G2 cells, although both of them bind to ASGPR that meditates the endocytosis. This is the first time, as far as we know, it has been demonstrated that the constitutional isomerism of sugars may bring different pathways and then different distributions of their nanoparticles inside the cell, although their internalizations are mediated by the same protein. Furthermore, since **NP-6-Gal** cannot reach the lysosome, it could be used as a better drug delivery system than **NP-1-Gal**.

■ ASSOCIATED CONTENT

Supporting Information

Synthesis, characterization, and self-assembly of **PF-1-Gal**, **PF-1-Man**, and **PF-6-Gal** including ^{1}H NMR and GPC results, as well as details of DLS and QCM measurements and cell imaging with Z-stack images (Figure S15, S16, S19, and S20). This material is available free of charge via the Internet at http://pubs.acs.org.

■ AUTHOR INFORMATION

Corresponding Authors

*E-mail: guosong@fudan.edu.cn.
*E-mail: yuding@fudan.edu.cn.

Notes

The authors declare no competing financial interest.

■ ACKNOWLEDGMENTS

Ministry of Science and Technology of China (2011CB932503332), National Natural Science Foundation of China (No. 91227203, 51322306), and the Shanghai Rising-Star Program (Grant 13QA1400600) are acknowledged for their financial support.

■ REFERENCES

(1) (a) Varki, A.; Cummings, R. D.; Esko, J. D.; Freeze, H. H. *Essentials of Glycobiology*, 2nd ed.; Cold Spring Harbor: NY, 2009. (b) Fleming, C.; Maldjian, A.; Costa, D. D.; Rullay, A. K.; Haddleton, D. M.; John, S. R.; Penny, P.; Noble, R. C.; Cameron, N. R.; Davis, B. G. *Nat. Chem. Biol.* **2005**, *1*, 270−274.
(2) Lee, Y. C.; Lee, R. T. *Acc. Chem. Res.* **1995**, *28*, 321−327.
(3) (a) Branson, T. R.; Turnbull, W. B. *Chem. Soc. Rev.* **2013**, *42*, 4613−4622. (b) Jiménez Blanco, J. L.; Ortiz Mellet, C.; Fernández, C. *Chem. Soc. Rev.* **2013**, *42*, 4518−4531. (c) Kiessling, L. L.; Grim, J. C. *Chem. Soc. Rev.* **2013**, *42*, 4476−4491. (d) Huang, J.; Bonduelle, C.; Thévenot, J.; Lecommandoux, S.; Heise, A. *J. Am. Chem. Soc.* **2012**, *134*, 119−122.
(4) (a) Bonduelle, C.; Huang, J.; Ibarboure, E.; Heise, A.; Lecommandoux, S. *Chem. Commun.* **2012**, *48*, 8353−8355. (b) Pfaff, A.; Shinde, V. S.; Lu, Y.; Wittemann, A.; Ballauff, M.; Müller, A. H. E. *Macromol. Biosci.* **2011**, *11*, 199−210. (c) Ting, S. R. S.; Min, E. H.; Escalé, P.; Save, M.; Billon, L.; Stenzel, M. H. *Macromolecules* **2009**, *42*, 9422−9434. (d) Godula, K.; Bertozzi, C. R. *J. Am. Chem. Soc.* **2012**, *134*, 15732−15742. (e) Pasparakis, G.; Cockayne, A.; Alexander, C. *J. Am. Chem. Soc.* **2007**, *129*, 11014−11015.
(5) (a) Kiessling, L. L.; Grim, J. C. *Chem. Soc. Rev.* **2013**, *42*, 4476−4491. (b) Gou, Y. Z.; Geng, J.; Richards, S. J.; Burns, J.; Becer, C. R.; Haddleton, D. M. *J. Polym. Sci., Part A: Polym. Chem.* **2013**, *51*, 2588−2597. (c) Zhang, Q.; Collins, J.; Anastasaki, A.; Wallis, R.; Mitchell, D. A.; Becer, C. R.; Haddleton, D. M. *Angew. Chem., Int. Ed.* **2013**, *52*, 4435−4439. (d) Xiong, Y. Y.; Li, Z. C.; Du, F. S.; Li, F. M. *Acta Polym. Sin.* **2001**, *6*, 787−792.
(6) Su, L.; Chen, G. S.; Jiang, M. *Polym. Chem.* **2012**, *3*, 1560−1566.
(7) Phillips, R. L.; Kim, I. B.; Carson, B. E.; Tidbeck, B.; Bai, Y.; Lowary, T. L.; Tolbert, L. M.; Bunz, U. H. F. *Macromolecules* **2008**, *41*, 7316−7320.
(8) Xue, C. H.; Luo, F. T.; Liu, H. Y. *Macromolecules* **2007**, *40*, 6863−6870.
(9) Xue, C. H.; Jog, S. P.; Murthy, P.; Liu, H. Y. *Biomacromolecules* **2006**, *7*, 2470−2474.
(10) Xu, W. D.; Lai, W. Y.; Fan, Q. L.; Huang, W. *Sci. Sin. Chim.* **2011**, *41*, 409−423.
(11) (a) Zhou, L.; Geng, J. L.; Wang, G.; Liu, J.; Liu, B. *ACS Macro Lett.* **2012**, *1*, 927−932. (b) Pu, K. Y.; Li, K.; Liu, B. *Adv. Funct. Mater.* **2010**, *20*, 2770−2777.
(12) Lu, S.; Fan, Q. L.; Chua, S. J.; Huang, W. *Macromolecules* **2003**, *36*, 304−310.
(13) Lian, X. M.; Wu, D. X.; Song, X. H.; Zhao, H. Y. *Macromolecules* **2010**, *43*, 7434−7445.
(14) Zhang, Q.; Slavin, S.; Jones, M. W.; Haddleton, A. J.; Haddleton, D. M. *Polym. Chem.* **2012**, *3*, 1016−1023.
(15) Roy, B.; Mukhopadhyay, B. *Tetrahedron Lett.* **2007**, *48*, 3783−3787.

(16) Aissou, K.; Pfaff, A.; Giacomelli, C.; Travelet, C.; Müller, A. H.; Borsali, R. *Macromol. Rapid Commun.* **2011**, *32*, 912−916.
(17) Wei, K. C.; Su, L.; Chen, G. S.; Jiang, M. *Polymer* **2011**, *52*, 3647−3654.
(18) (a) Banerjee, R.; Das, K.; Ravishankar, R.; Suguna, K.; Surolia, A.; Vijayan, M. *J. Mol. Biol.* **1996**, *259*, 281−296. (b) Ravishankar, R.; Thomas, C. J.; Suguna, K.; Surolia, A.; Vijayan, M. *Protein* **2001**, *43*, 260−270.
(19) (a) Svensson, C.; Teneberg, S.; Nilsson, C. L.; Kjellberg, A.; Schwarz, F. P.; Sharon, N.; Krengel, U. *J. Mol. Biol.* **2002**, *321*, 69−83. (b) Turton, K.; Natesh, R.; Thiyagarajan, N.; Chaddock, J. A.; Acharya, K. R. *Glycobiology* **2004**, *14*, 923−929.
(20) (a) Lai, C. H.; Lin, C. Y.; Wu, H. T.; Chan, H. S.; Chuang, Y. J.; Chen, C. T.; Lin, C. C. *Adv. Funct. Mater.* **2010**, *20*, 3948−3958. (b) He, X. L.; Wang, J. Y.; Xiao, F.; Cheng, L. *Acta Polym. Sin.* **2009**, *12*, 1274−1281.
(21) Rigopoulou, E. I.; Roggenbuck, D.; Smyk, D. S.; Liaskos, C.; Mytilinaiou, M. G.; Feist, E.; Conrad, K.; Bogdanos, D. P. *Autoimmun. Rev.* **2012**, *12*, 260−269.
(22) Eisele, N. B.; Andersson, F. I.; Frey, S.; Richter, R. P. *Biomacromolecules* **2012**, *13*, 2322−2332.
(23) (a) Mamidyala, S. K.; Dutta, S.; Chrunyk, B. A.; Préville, C.; Wang, H.; Withka, J. M.; et al. *J. Am. Chem. Soc.* **2012**, *134*, 1978−1981. (b) Kolatkar, A. R.; Weis, W. I. *J. Biol. Chem.* **1996**, *271*, 6679−6685.
(24) Tian, X. Z.; Pai, J. Y.; Baek, K. H.; Ko, S. K.; Shin, I. *Chem. Asian J.* **2011**, *6*, 2107−2113.
(25) Basiruddin, S. K.; Maity, A. R.; Jana, N. R. *RSC Adv.* **2012**, *2*, 11915−11921.
(26) Tian, X. Z.; Baek, K. W.; Shin, I. *Mol. BioSyst.* **2013**, *9*, 978−986.
(27) Lee, M. H.; Han, J. H.; Kwon, P. S.; Bhuniya, S.; Kim, J. Y.; Sessler, J. L.; Kang, C.; Kim, J. S. *J. Am. Chem. Soc.* **2012**, *134*, 1316−1322.